Nanoparticle–Protein Assembly

DOI: 10.1002/anie.200701180

Assembly of Nanoparticle–Protein Binding Complexes: From Monomers to Ordered Arrays**

*Minghui Hu, Luping Qian, Raymond P. Briñas, Elena S. Lymar, and James F. Hainfeld**

Nanoparticle (NP)–biomolecule binding complexes have shown promising applications in imaging, sensing, catalysis, electronics, and cell targeting because NPs possess size-dependent optical, electrical, and magnetic properties while biomolecules can perform unique biological functionalities.[1] NP–biomolecule hybrid structures with various architectures have been constructed by using biomolecules as templates.[2] Meanwhile, the site-specific recognition has been extensively employed for many applications that require biomolecule structural control.[3] Although biomolecules themselves show versatile assembling properties,[4] NPs have been used as templates to construct NP–biomolecule binding complexes through interactions with DNA,[5] proteins,[6] and viral capsids.[7] However, the potential of functionalized NPs as templates to assemble proteins has not been fully explored, and the control of NP–protein nanostructures remains challenging.

Herein, we report the formation of NP–protein hybrid complexes with controlled geometry, stoichiometry, orientation, and specificity by tailoring the sizes of binding NPs and placement of genetic tags in proteins. Well-defined NP–protein complexes are formed through site-specific binding between 6×histidine (His) tags in proteins and nickel-nitrilotriacetic acid (Ni-NTA) functional groups on Au NPs with sizes ranging from 1 to 4 nm. Our study demonstrates that NPs are not only appealing templates for assembling functional biomolecules, but also provide a mortar to construct novel geometrical and topological architectures of hybrid NP–protein complexes.

In this study, we synthesized a ligand-containing NTA moiety, (1*S*)-*N*-[5-[(4-Mercaptobutanoyl)amino]-1-carboxypentyl]iminodiacetic acid (NTA-Lys-SH) (see Scheme S1 in the Supporting Information).[8] This ligand was used to synthesize 1.3-nm NTA Au NPs from $Au(PPh_3)_8Cl_3$ (see Scheme S2 and Figure S1 in the Supporting Information)[9] and 4.4-nm NTA Au NPs from $HAuCl_4$ (see Scheme S3 and Figure S2 in the Supporting Information) followed by reaction with a solution of $NiCl_2$ to form Ni-NTA Au NPs. We used these NPs as templates to assemble two 6×His-tagged proteins, an adenovirus serotype 12 (Ad12) knob,[10] and a mycobacterium tuberculosis (Mtb) 20S proteasome.[11] In the 60-kDa C_3-symmetric knob protein, a 6×His tag was fused onto the N terminus of each subunit, forming a highly localized binding motif (Figure 1a). The 750-kDa D7-symmetric proteasome protein has a stack of four rings, αββα, and each layer has seven identical subunits. A 6×His tag was fused onto the C terminus of each β subunit, thus creating seven pairs of binding motifs that are uniformly dispersed around the periphery of the two central layers (Figure 1b).

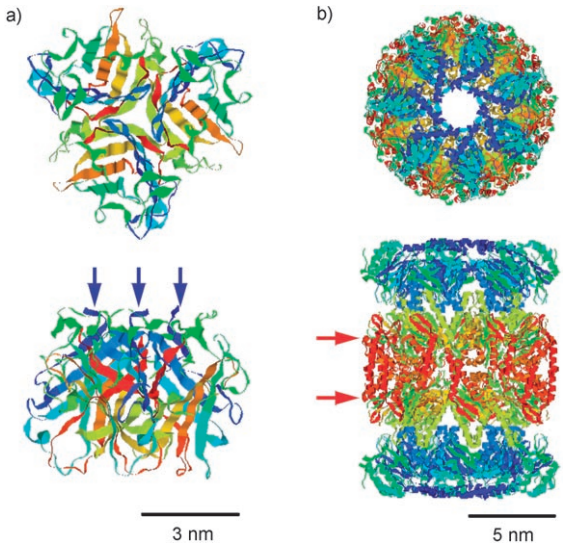

Figure 1. 3D structures of Ad12 knob and 20S proteasome proteins showing the binding motif to Au NPs. a) Knob protein[10] in which a 6×His tag (indicated by the arrow) is attached to the N terminus of each subunit; b) proteasome protein[11] in which a 6×His tag (indicated by the arrow) is attached to the C terminus of each of the fourteen β subunits around the central equator.

For the Ad12 knob, the close proximity of the three 6×His tags favored the formation of monomers, dimers, trimers, and three-dimensional (3D) spherical shells on Au NPs with sizes ranging from 1 to 4 nm. The knob protein solution was mixed with 1.3-nm Au NPs, followed by separation by using size-exclusion chromatography (SEC; Figure 2). Two major fractions at 32.0 and 37.4 min were collected, both of which showed the absorption characteristics of 1.3-nm Au NPs (continuously from 200–500 nm) and proteins (280 nm; see Figure S4 in the Supporting Information). High-angle annular dark field (HAADF) scanning transmission electron micro-

[*] Dr. M. Hu, L. Qian, Dr. R. P. Briñas, Dr. E. S. Lymar, Dr. J. F. Hainfeld
Biology Department
Brookhaven National Laboratory
Upton, NY 11973 (USA)
Fax: (+1) 631-3443407
E-mail: hainfeld@bnl.gov

[**] This work was supported by BNL LDRD Grant 04-055, DOE Grant 06742, and NIH Grants P41EB002181 and R01RR017545. We thank Y. Zhang, P. I. Freimuth, G. Hu, H. Li, and C. F. Nathan for kindly providing protein samples, and J. S. Wall, M. Simon, B. Lin, and F. Kito for assistance with STEM analysis.

Supporting information for this article is available on the WWW under http://www.angewandte.org or from the author.

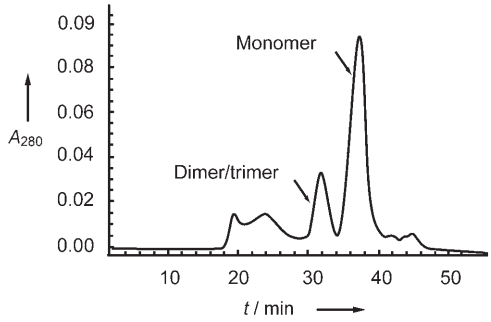

Figure 2. Size-exclusion-chromatography profile of binding complexes of 6×His-tagged Ad12 knob proteins and 1.4-nm Ni-NTA Au NPs showing separation of the monomer and dimer (occasional trimer). A_{280} = absorbance at 280 nm.

scopy (STEM) analysis indicated that the fraction at 32 min was protein monomers on Au NPs with an average size of 0.8 nm (Figure 3a,d), whereas the fraction at 37 min was mainly protein dimers on Au NPs with an average size of 1.6 nm (Figure 3b,e). A few trimers on larger NPs were found in the dimer fraction (Figure 3b,f). When 4.4-nm Au NPs were used, 3D NP–protein core-shell complexes were formed instead of discrete numbers of the protein (Figure 3c,g). In the presence of excess proteins, all of the Au NPs were encapsulated by proteins, showing a high binding efficiency. This structural dependence on the NP size appears to result from the surface area available for protein binding.[5b,6a]

For the 20S proteasome, the dispersed distribution of 6× His tags resulted in the formation of two-dimensional (2D) ordered tetragonal arrays with a 1:1 stoichiometry instead of 3D spherical shells. Here, we used 3.7-nm Au NPs with a narrower size deviation of 0.7 nm, which were isolated by centrifugation of 4.4-nm NPs (see Figure S3 in the Supporting Information). The formation of ordered tetragonal arrays over several hundred nanometers has been observed (Figure 4a). As predicted from the position of 6×His tags in the proteasome protein (Figure 1b), NPs bound exactly to the central equator of cylindrical proteasome (Figure 4b,c). Study in situ by using cryogenic (cryo)-TEM confirmed the formation of tetragonal NP–protein arrays in the solution (Figure 5). The size of Au NPs in the arrays had a lower deviation than that of as-used arrays (see Figure S3 in the Supporting Information). This could result from size selection during the array growth in which more identical NPs are incorporated into the arrays. An averaged image over multiple protein molecules in an array revealed a top view of the cylindrical structure of 20S proteasomes. This architectural formation can be understood from the steric restriction based on the Pauling's rules (see Table S1 in the Supporting Information).[12]

When 6×His tags were removed from a thrombin cleavage site in Ad12 knob and 20S proteasome proteins, these proteins showed no binding to Ni-NTA Au NPs (Figure 6). This is indicative of the highly specific interactions between these Au NPs and proteins.

These results demonstrate that NP–protein binding complexes can be constructed with predictable architecture by tailoring NP size, functionality, and placement of genetic tags.

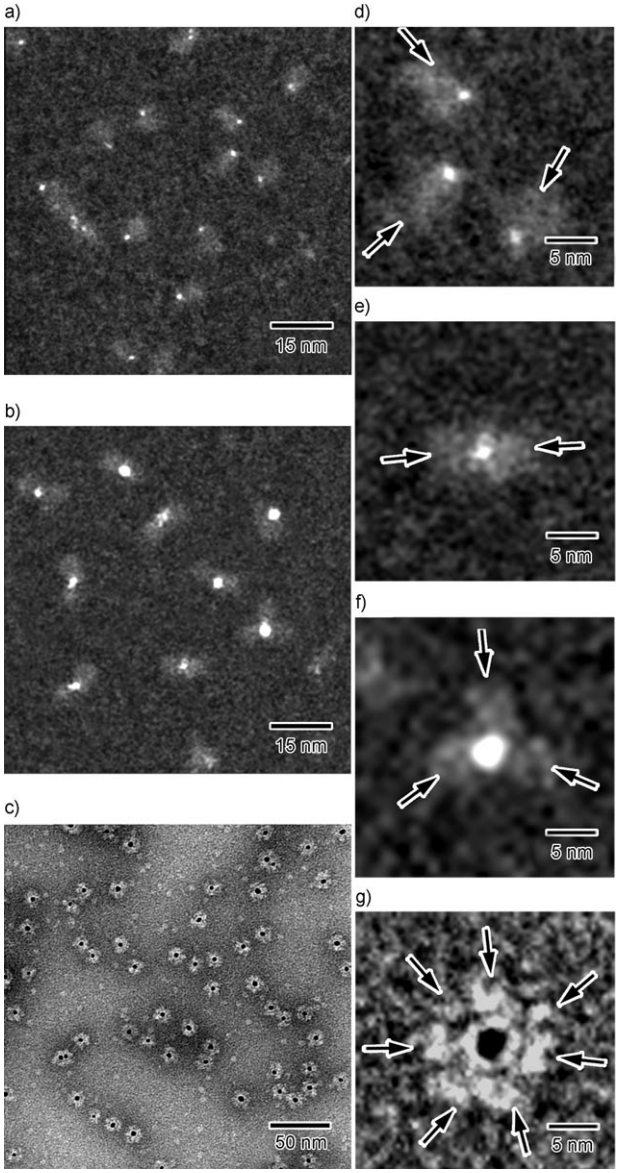

Figure 3. TEM images of monomers, dimers, trimers, and core-shell assemblies of Ad12 knob proteins and Au NPs with different sizes. HAADF STEM images of a) monomer and b) dimer/trimer of 6×His-tagged Ad12 knob proteins attached to 1.4-nm Au NPs, which were isolated by using size-exclusion chromatography; c) negative-stain TEM image of core-shell binding complexes of knob proteins with 4.4-nm NPs; d)–g) close-up view of monomers, dimers, trimers, and 3D spherical shells, respectively, in which each knob molecule is marked by an arrow.

Taking the Ad12 knob and Mtb 20S proteasome proteins as examples, monomers, dimers, trimers, 3D spherical shells, and 2D ordered arrays are formed. These hybrid structures formed by coupling NPs and proteins are promising for novel applications. The knob protein is typically found on the end of viral spikes and mediates adenovirus attachment and uptake through a high binding affinity with the coxsackie and adenovirus receptor (CAR) on the surface of many cell types.[10] The NP–knob binding complexes potentially enable visualization of cellular attachment and nanoparticle delivery. The proteasome protein is involved in mycobacterial defence

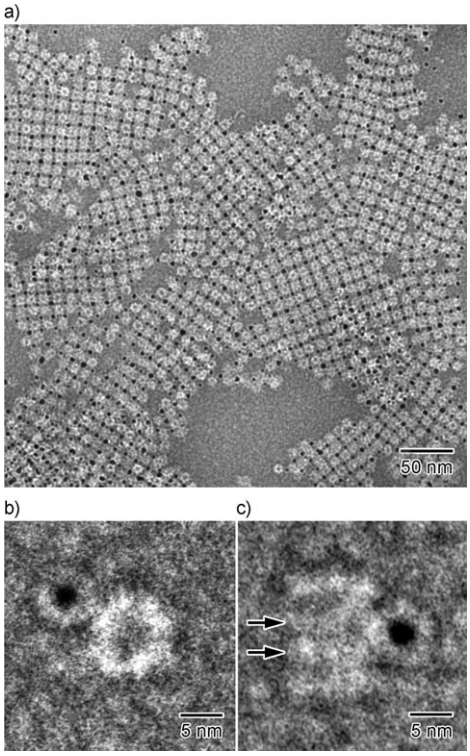

Figure 4. Negative-stain TEM images of binding complexes of 3.7-nm Au NPs and 20S proteasome proteins. a) NP–proteasome 2D arrays; b) top and c) side view of a proteasome protein bound to an Au NP in which the two innersubunit β rings are indicated by the arrows.

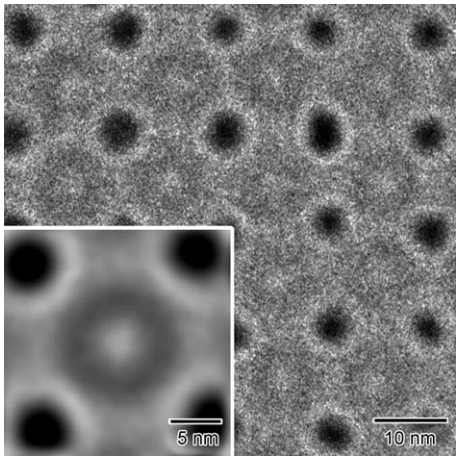

Figure 5. Cryo-TEM images of tetragonal arrays of 3.7-nm Au NPs and 20S proteasome proteins with a stoichiometry of 1:1. The inset shows an averaged image over multiple protein molecules in an array.

against host nitrosative stress.[11] The enzyme activity may be modulated upon binding to Au NPs. The formation of 2D NP–protein arrays might improve alignment and enhance resolution in cryo-electron microscopy structural studies.

Received: March 17, 2007
Published online: May 30, 2007

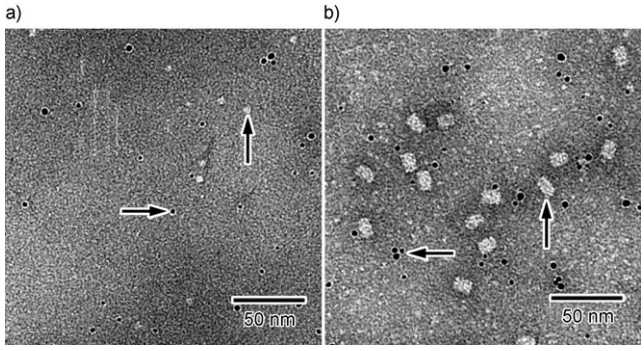

Figure 6. Negative-stain TEM images of Au NPs with a) Ad12 knob and b) 20S proteasome proteins whose 6×His tags were removed and therefore showed no formation of binding complexes.

Keywords: electron microscopy · hybrid materials · nanoparticles · proteins · self-assembly

[1] a) L. Montesano-Roditis, D. G. Glitz, R. R. Traut, P. L. Stewart, *J. Biol. Chem.* **2001**, *276*, 14117–14123; b) Y. Xiao, F. Patolsky, E. Katz, J. F. Hainfeld, I. Willner, *Science* **2003**, *299*, 1877–1881; c) L. Bumba, M. Tichy, M. Dobakova, J. Komenda, F. Vacha, *J. Struct. Biol.* **2005**, *152*, 28–35; d) C. You, S. S. Agasti, M. De, M. J. Knapp, V. M. Rotello, *J. Am. Chem. Soc.* **2006**, *128*, 14612–14618; e) R. J. Tseng, C. Tsai, L. Ma, J. Ouyang, C. S. Ozkan, Y. Yang, *Nat. Nanotechnol.* **2006**, *1*, 72–77; f) D. C. Deniger, A. A. Kolokoltsov, A. C. Moore, T. B. Albrecht, R. A. Davey, *Nano Lett.* **2006**, *6*, 2414–2421.

[2] a) M. Allen, D. Willits, J. Mosolf, M. Young, T. Douglas, *Adv. Mater.* **2002**, *14*, 1562–1565; b) D. Ishii, K. Kinbara, Y. Ishida, N. Ishii, M. Okochi, M. Yohda, T. Aida, *Nature* **2003**, *423*, 628–632; c) R. Djalali, Y. Chen, H. Matsui, *J. Am. Chem. Soc.* **2002**, *124*, 13660–13661; d) R. A. McMillan, C. D. Paavola, J. Howard, S. L. Chan, N. J. Zaluzec, J. D. Trent, *Nat. Mater.* **2002**, *1*, 247–252; e) A. S. Blum et al., *Nano Lett.* **2004**, *4*, 867–870; f) R. Baron, B. Willner, I. Willner, *Chem. Commun.* **2007**, 323–332.

[3] a) K. K. Caswell, J. N. Wilson, U. H. F. Bunz, C. J. Murphy, *J. Am. Chem. Soc.* **2003**, *125*, 13914–13915; b) C. M. Niemeyer, W. Burger, J. Peplies, *Angew. Chem.* **1998**, *110*, 2391–2395; *Angew. Chem. Int. Ed.* **1998**, *37*, 2265–2268; c) J. F. Hainfeld, W. Liu, C. M. R. Halsey, P. Freimuth, R. D. Powell, *J. Struct. Biol.* **1999**, *127*, 185–198; d) M. Aubin, D. G. Morales, K. Hamad-Schifferli, *Nano Lett.* **2005**, *5*, 519–522.

[4] a) T. O. Yeates, J. E. Padilla, *Curr. Opin. Struct. Biol.* **2002**, *12*, 464–470; b) P. Ringler, G. E. Schulz, *Science* **2003**, *302*, 106–109; c) L. Nasalean, S. Baudrey, N. B. Leontis, L. Jaeger, *Nucleic Acids Res.* **2006**, *34*, 1381–1392; d) J. C. T. Carlson, S. S. Jena, M. Flenniken, T. Chou, R. A. Siegel, C. R. Wagner, *J. Am. Chem. Soc.* **2006**, *128*, 7630–7638; e) K. Sugimoto, S. Kanamaru, K. Iwasaki, F. Arisaka, I. Yamashita, *Angew. Chem.* **2006**, *118*, 2791–2794; *Angew. Chem. Int. Ed.* **2006**, *45*, 2725–2728; f) S. Ghosh, M. Reches, E. Gazit, S. Verma, *Angew. Chem.* **2007**, *119*, 2048–2050; *Angew. Chem. Int. Ed.* **2007**, *46*, 2002–2004.

[5] a) F. Patolsky, Y. Weizmann, O. Lioubashevski, I. Willner, *Angew. Chem.* **2002**, *114*, 2429–2433; *Angew. Chem. Int. Ed.* **2002**, *41*, 2323–2327; b) C. J. Ackerson, M. T. Sykes, R. D. Kornberg, *Proc. Natl. Acad. Sci. USA* **2005**, *102*, 13383–13385; c) S. J. Hurst, A. K. R. Lytton-Jean, C. A. Mirkin, *Anal. Chem.* **2006**, *78*, 8313–8318.

[6] a) A. A. Vertegel, R. W. Siegel, J. S. Dordick, *Langmuir* **2004**, *20*, 6800–6807; b) F. Patolsky, Y. Weizmann, I. Willner, *Nat. Mater.* **2004**, *3*, 692–695; c) S. Srivastava, A. Verma, B. L. Frankamp, V. M. Rotello, *Adv. Mater.* **2005**, *17*, 617–621.

[7] a) L. Loo, R. H. Guenther, V. R. Basnayake, S. A. Lommel, S. Franzen, *J. Am. Chem. Soc.* **2006**, *128*, 4502 – 4503; b) C. Chen et al., *Nano Lett.* **2006**, *6*, 611 – 615.
[8] O. Du Roure, C. Debiemme-Chouvy, J. Malthete, P. Silberzan, *Langmuir* **2003**, *19*, 4138 – 4143.
[9] G. H. Woehrle, M. G. Warner, J. E. Hutchison, *J. Phys. Chem. B* **2002**, *106*, 9979 – 9981.
[10] M. C. Bewley, K. Springer, Y. Zhang, P. Freimuth, J. M. Flanagan, *Science* **1999**, *286*, 1579 – 1583.
[11] G. Q. Hu, G. Lin, M. Wang, L. Dick, R. Xu, C. Nathan, H. L. Li, *Mol. Microbiol.* **2006**, *59*, 1417 – 1428.
[12] L. Pauling, *J. Am. Chem. Soc.* **1929**, *51*, 1010 – 1026.

